AD-A081 958 JAYCOR ALEXANDRIA VA F/6 20/7
INVESTIGATION OF COLLECTION ION ACCELERATION USING INTENSE RELA--ETC(U)
FEB 80 F MAKO N00173-79-C-0808
UNCLASSIFIED JAYCOR-320-80-002-FR NL

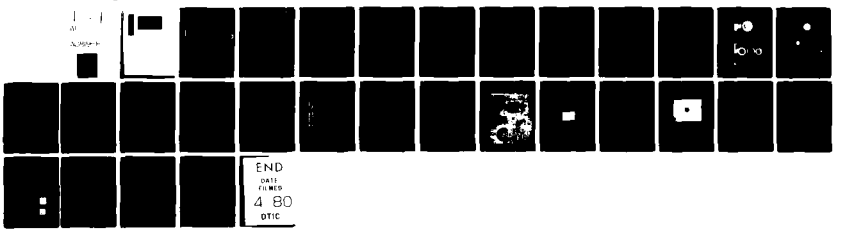

END
DATE FILMED
4 80
DTIC

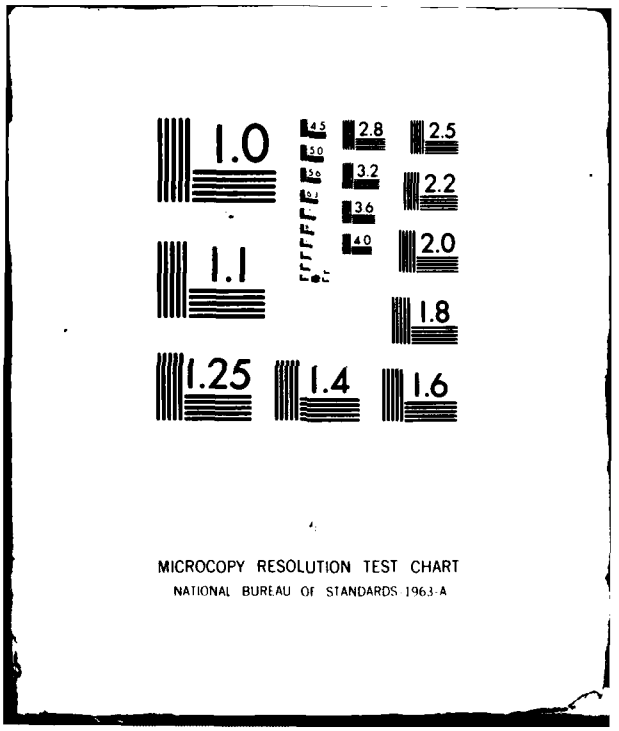
1.0
1.1
1.25
1.4
1.6
1.8
2.0
2.2
2.5
2.8
3.2
3.6
4.0
4.5
5.0
5.6
MICROCOPY RESOLUTION TEST CHART
NATIONAL BUREAU OF STANDARDS 1963-A

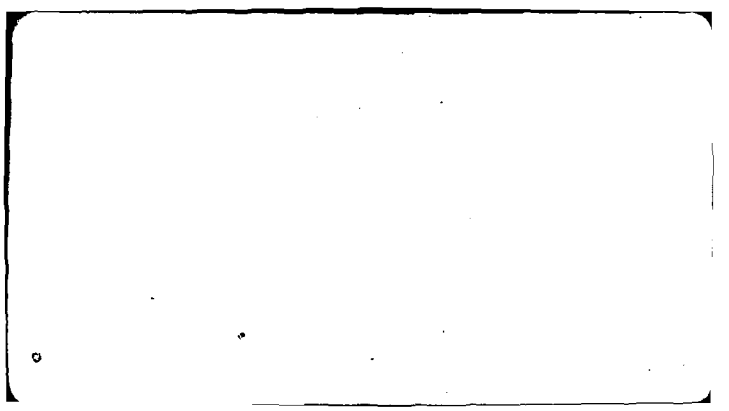

(6) INVESTIGATION OF COLLECTION ION ACCELERATION USING INTENSE RELATIVISTIC ELECTRON BEAMS.

(9) Final rept. 11 Dec 78 - 12 Dec 79,

(1) Frederick/Mako

JAYCOR Project No. 6132

(15) Contract No. N00173-79-C-0408

Final Report No. 320-80-002-FR

(12) 30

(11) February 1980

(14) JAYCOR-320-80-002-FR

205 S. Whiting Street
Alexandria, VA. 22304

Submitted to:

Naval Research Laboratory
Washington, DC 20375

393453

JOB

UNCLASSIFIED

SECURITY CLASSIFICATION OF THIS PAGE (When Data Entered)

REPORT DOCUMENTATION PAGE		READ INSTRUCTIONS BEFORE COMPLETING FORM
1. REPORT NUMBER 320-80-002-FR	2. GOVT ACCESSION NO.	3. RECIPIENT'S CATALOG NUMBER
4. TITLE (and Subtitle) Investigation of Collection Ion Acceleration Using Intense Relativistic Electron Beams		5. TYPE OF REPORT & PERIOD COVERED Final Report 12-11-78 - 12-13-79 6. PERFORMING ORG. REPORT NUMBER 320-80-002-FR/Project #6132
7. AUTHOR(s) Frederick Mako		8. CONTRACT OR GRANT NUMBER(s) N00173-79-C-0408
9. PERFORMING ORGANIZATION NAME AND ADDRESS JAYCOR 205 S. Whiting Street Alexandria, VA 22304		10. PROGRAM ELEMENT, PROJECT, TASK AREA & WORK UNIT NUMBERS
11. CONTROLLING OFFICE NAME AND ADDRESS Naval Research Laboratory Washington, DC 20375		12. REPORT DATE February 1980 13. NUMBER OF PAGES 28
14. MONITORING AGENCY NAME & ADDRESS(if different from Controlling Office)		15. SECURITY CLASS. (of this report) UNCLASSIFIED 15a. DECLASSIFICATION/DOWNGRADING SCHEDULE

16. DISTRIBUTION STATEMENT (of this Report)

Code 6701
Code 6702
Code 6740
Code 2627
DDC

17. DISTRIBUTION STATEMENT (of the abstract entered in Block 20, if different from Report)

18. SUPPLEMENTARY NOTES

19. KEY WORDS (Continue on reverse side if necessary and identify by block number)

20. ABSTRACT (Continue on reverse side if necessary and identify by block number)

DD FORM 1 JAN 73 1473 EDITION OF 1 NOV 65 IS OBSOLETE

UNCLASSIFIED

SECURITY CLASSIFICATION OF THIS PAGE (When Data Entered)

CONTENTS

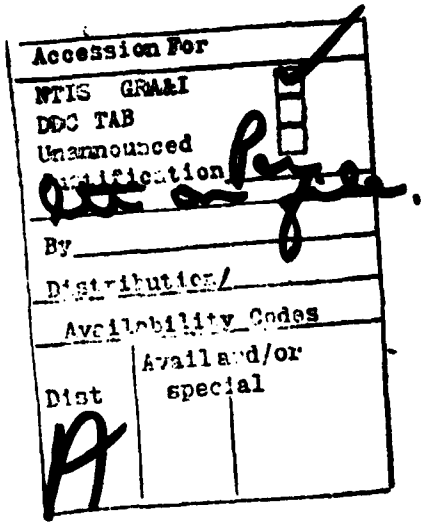

I. INTRODUCTION

Recently there has been an increased interest in a compact high energy intense light-ion accelerator. Some of the areas of application for such an accelerator include directed energy research, inertial fusion and magnetic fusion. The range of desired properties for the ion beam are an energy of from .1 to 1 GeV and an intensity of from 10^{13} to 10^{16} ions/cm^2 per pulse, where the pulse length can be from less than one nanosecond to a millisecond. A compact accelerator refers to the longest length being from 10 to 30 meters.

A technological breakthrough in the generation of intense relativistic electron beams (IREB) has made the above type of ion accelerator realizable. The property of an intense relativistic electron beam which makes it useful for ion acceleration is being able to produce an electric field strength of about 1 MV/cm in the beam. As a comparison, conventional accelerators produce an electric field with a strength of about .01 MV/cm. Although many approaches exist for attaining the acceleration of positive ions via the collective electric field produced by an intense relativistic electron beam, not all approaches can be scaled-up to high ion energies. Scaleability means there is a systematic procedure for maintaining synchronization between the accelerating ion and the accelerating electrostatic potential well that is pushing the ion. The requirement of scaleability is one general to any type of accelerator.

Only modest progress has been made in the last decade on the scaleable schemes for accelerating positive ions using an IREB. It is not clear what the exact reason is for the lack of progress, however, from the large

amount of time spent thus far, it is clear that a new approach is necessary.

The new approach that has been proposed for investigation ~~by NRL and JAYCOR~~ is the space charge wave accelerator.

With the space charge wave type of collective ion acceleration scheme, one can expect a compact, efficient ion accelerator which is capable of producing high energy and high current ion beams. The ion energy limit occurs when the ion velocity equals that of the electrons. Thus, for an easily producible 1 MeV electron beam about 2 GeV protons are expected. Since a large number of electrons are needed for an intense relativistic electron beam, a proportional but smaller number of ions are expected by momentum balance. With an accelerating electric field having a strength of 1 MV/cm, the 2 GeV protons can be obtained in a short accelerator length of 20 meters.

The space charge wave ion accelerator has great expectations. It is, however, not without problems. The most important problem is that of matching the ion and wave velocity. It appears technically difficult to slow the phase velocity of the fundamental mode of a space charge wave on an IREB to below .2 to .3 times the speed of light. At these velocities a proton would have to have an energy of 16 to 30 MeV respectively. And, intense (1 kA) medium energy (30 MeV) proton sources do not exist as yet. The problem of velocity matching has two approaches suggested: (1) development of an intense energetic ion source and (2) develop a means for controlling the wave phase velocity. The next two sections present the progress thus far on the above two approaches.

The next section presents the current development of an intense ion injector and references Appendix A on a completed injector scheme. The last section shows the present status of the wave accelerator and presents the final results of a theoretical study on a periodic structure for producing low phase velocities. Reference B presents a detailed theoretical study on the periodic wave accelerator. This is a potential injector scheme.

II. INTENSE ION INJECTORS

In order to use an ion injector with a wave accelerator several criteria must be met. The first of course is being able to reach an energy of 30 MeV for protons in order to insure loading of the ions into the wave accelerator. Not only must the ion and wave velocity match in magnitude but they must also be in the same direction. This creates two more conditions, namely the bulk of the ion beam must be traveling in the wave direction. In addition, the ions must be focussed such that the ion and wave velocity vectors are colinear. The final condition is that the injector must be capable of repetitive operation. This condition reduces contamination. Typically in a single shot operation the vacuum system must be opened and closed after every shot. In addition, the rep-rate condition allows rapid data acquisition. This makes possible definitive experiments.

In Appendix A an injector is described which shows a factor of 7 in ion energy multiplication above the electron energy. In addition, the energetic ions are directed and confined to the electron beam diameter. However, the number of accelerated ions/pulse is too small to be of interest. The low ion intensity is primarily a result of using a low pressure gas to extract ions from. Also, it is not clear how to increase the ion energy up to the required minimum wave phase velocity. And finally, the system cannot be repetitively operated since a foil is required to isolate gas from the diode region.

Most of these deficiencies are surmounted in the present work. Experimental results from a foilless ion diode (Fig. 1) capable of repetitive pulsing are presented. More than 10^{14} protons/pulse are observed in a foilless reflexing configuration using an 800 kV, 20 kA, 50 ns long electron beam in a 20 kG magnetic field. Both insulating (polyethylene) and conducting

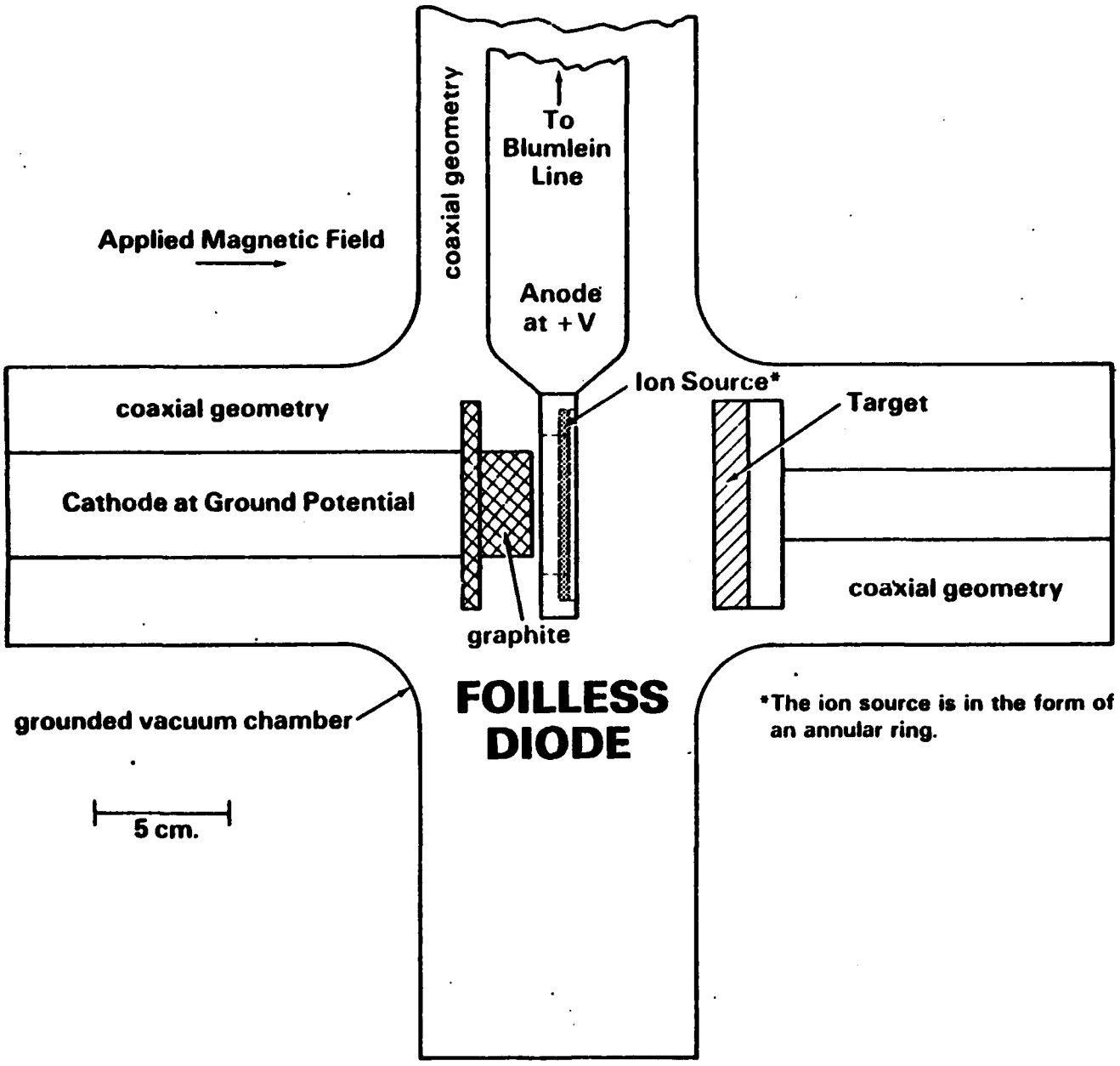
coaxial geometry
To Blumlein Line
Applied Magnetic Field
Anode at +V
Ion Source*
Target
coaxial geometry
Cathode at Ground Potential
coaxial geometry
graphite
FOILLESS DIODE
*The ion source is in the form of an annular ring.
grounded vacuum chamber
5 cm.

Figure 1

(H_2 and D_2 loaded Ti) anodes are used. Targets used were graphite and stacks of 12.5 μm of polyethylene foils.

Figure 2 shows photographs of the anode structure. Figure 2A is a stainless steel housing which is insulated by macor from the H_2 loaded titanium ion source. Figure 2B is a photograph of the disassembled anode structure. Figure 3 shows photographs of the graphite target. The graphite target and activation analysis is used to determine the radial proton distributions. In Figure 4 each measurement has been averaged over three shots. The ion beam changes from a hollow beam with a diameter of approximately that of the ion source at an axial position of 5 cm to a focussed beam at 15 cm from the anode. Figure 5 shows how tightly focussed the ion beam becomes at 15 cm. The beam focusses to a radius of about 1 cm. The very small graphite rings (Fig. 3c) were used in this determination. Figure 6 is a plot which shows a measure of the accelerated deuteron distribution. The number of deuterons in the second foil is two orders of magnitude lower than the first. The energy of the ions stopped within the first foil is less than 1 MeV. The directionality of accelerated ions is four times greater in the forward direction. That is there are four times as many ions traveling to the target (Fig. 1) than to the cathode.

This scheme satisfies almost all of the criteria set down at the beginning of this section. The only deficiency is that the ion energy is too low for direct injection into a wave accelerator. One solution to this problem is to stage the ion sources. By reversing the polarity of the present configuration, i.e., grounding the anode and setting the cathode at a negative potential it is then possible to add more ion sources at ground potential. The sources are axially separated in the direction of beam propagation. The ion sources are initiated externally and timed to insure

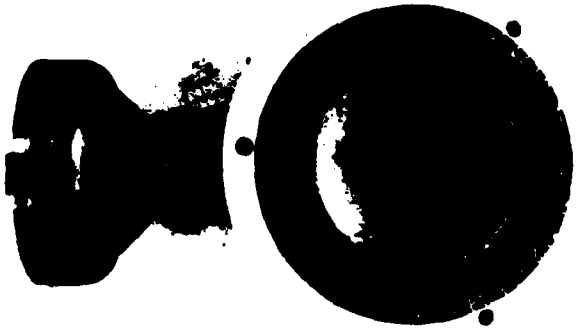

A

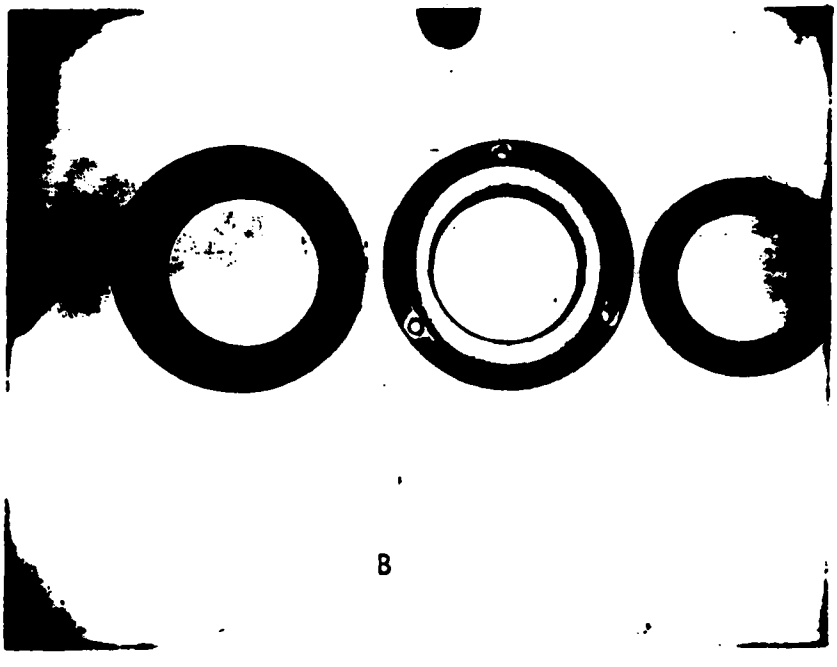

B

Figure 2. ANODE

A. Assembled with Macor Insulator and H_2 Loaded Titanium Ion Source.

B. Disassembled.

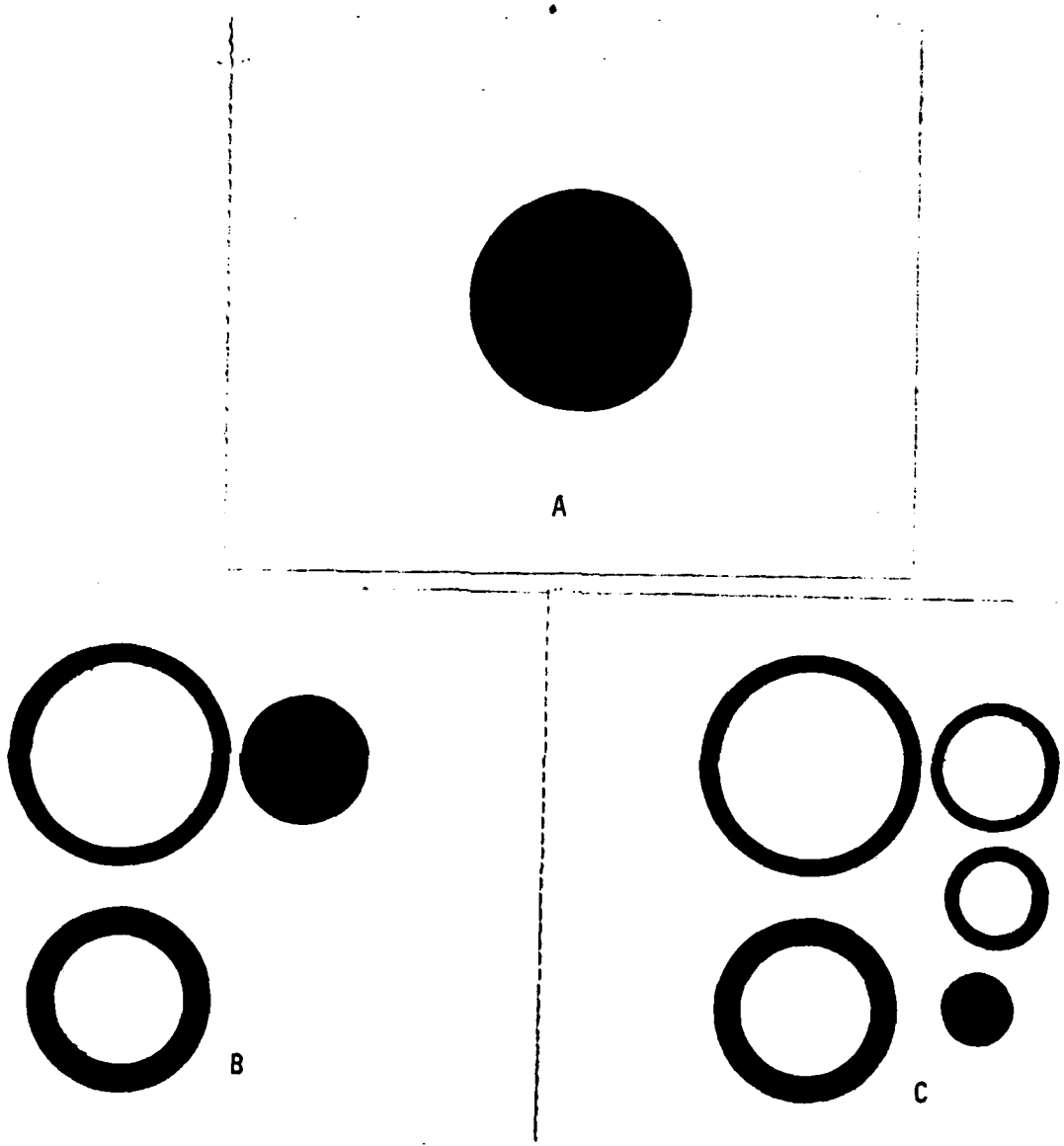

Figure 3. GRAPHITE TARGET

A. Assembled Target. The diameter is 7.5 cm.

B. Target disassembled into three equal area sections.

C. The target with the center section disassembled into three equal area sections.

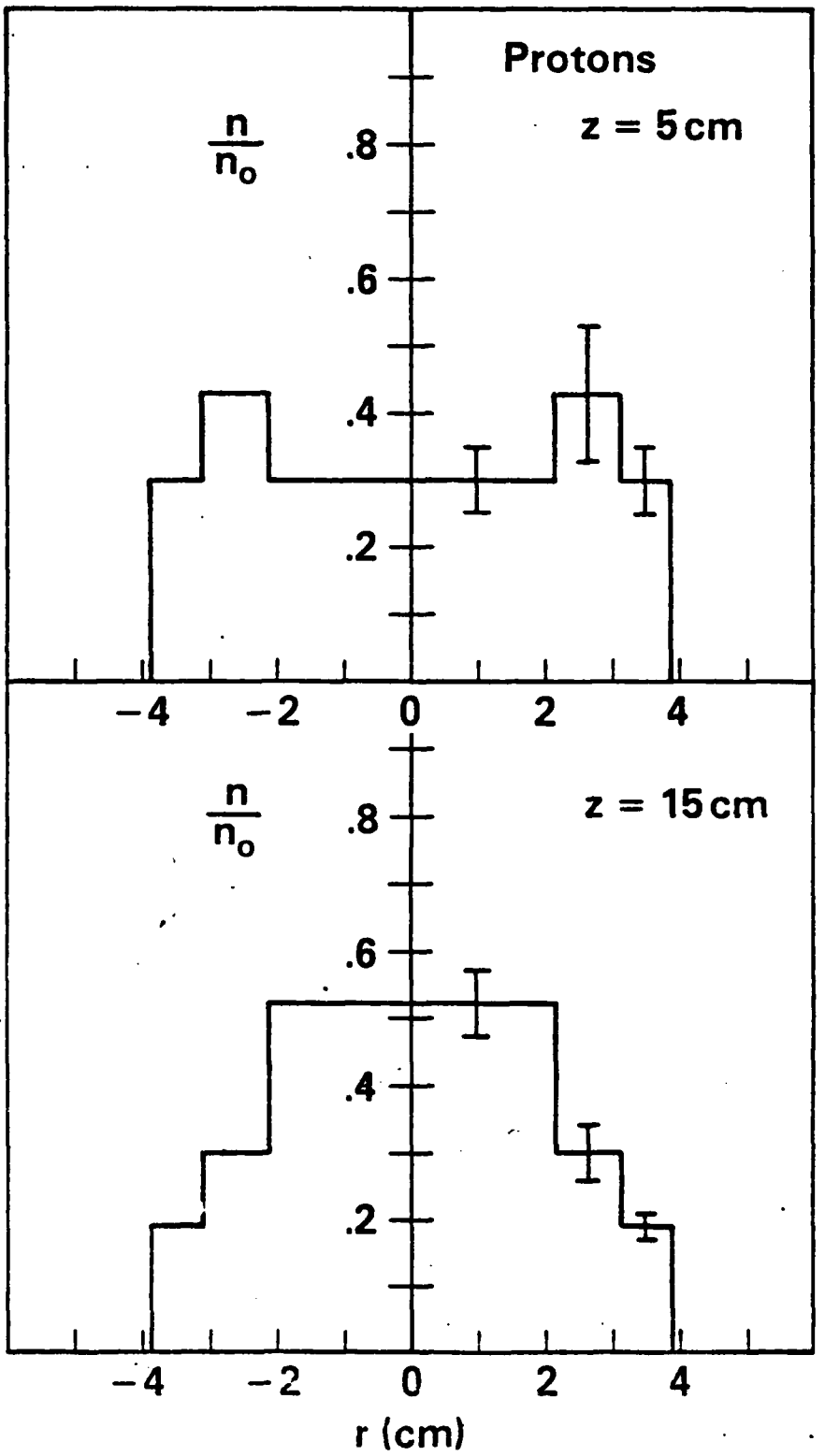

Figure 4

Radial Distribution of Protons at Different Axial Positions

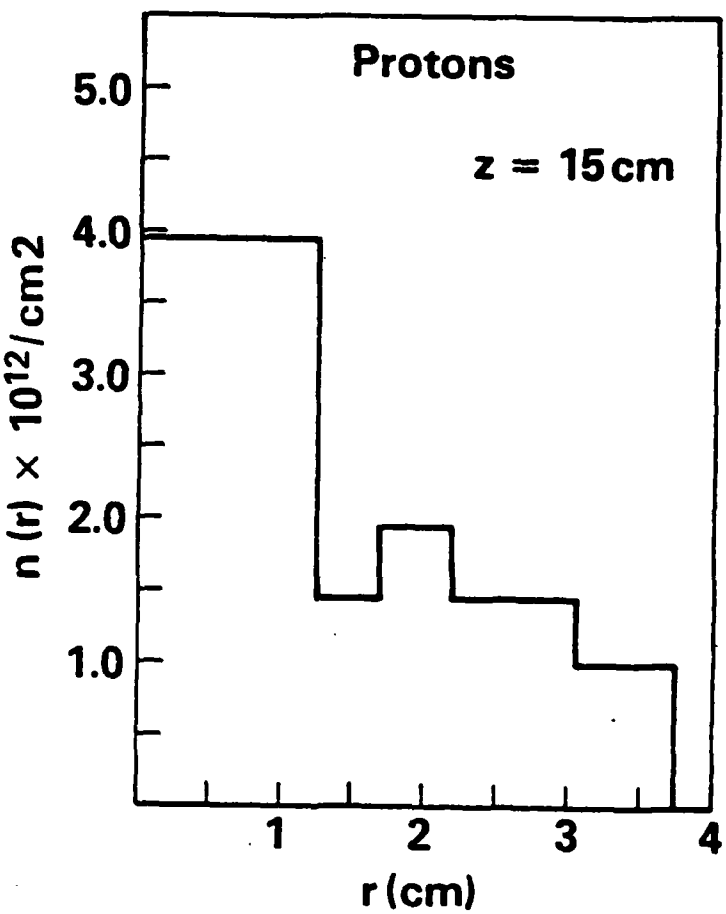

Figure 5

Refined Radial Proton Distribution

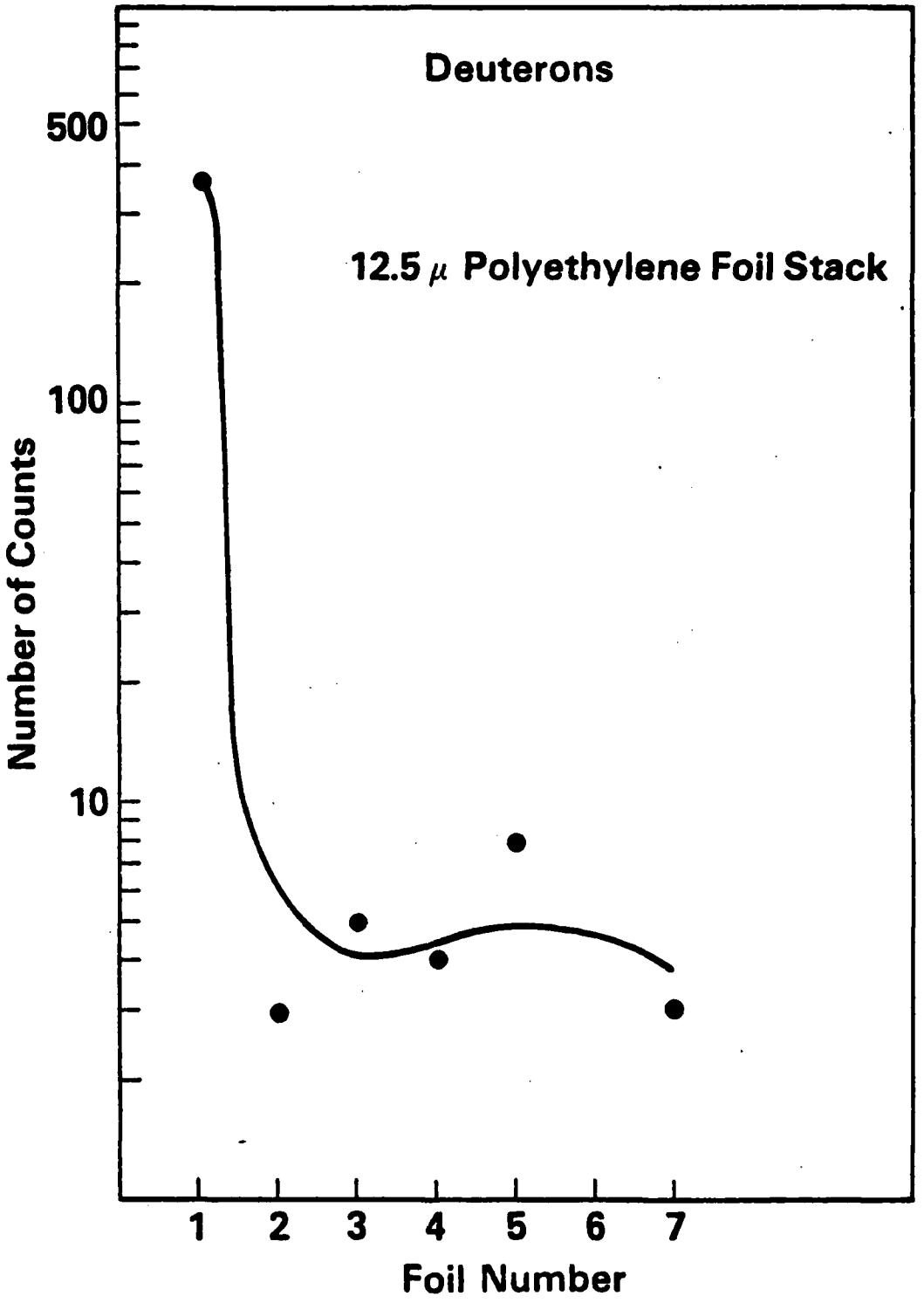

Figure 6

Deuteron Energy Distribution

synchronous ion acceleration with the electron beam front. In this way, further energy may be gained by the ions. This approach is going to be studied by computer simulation to investigate whether it will be feasible for an experimental study.

III. WAVE ACCELERATOR

NRL has proposed a solution to the wave phase velocity problem. The solution is a pre-space charge wave accelerator. This scheme can take ions from 1 MeV to 30 MeV. This accelerator is based on exciting higher order spatial harmonics of a variable period slow wave structure. The phase-velocity of the first harmonic can have a value near zero. A detailed theoretical study has been carried out in Appendix B. From this analysis it appears technically unfeasible to use higher order modes. The magnitude of the accelerating electric field for the first harmonic is about 1/5 as large as the field of the fundamental mode. In addition, in order for ions to be accelerated by the above electric field, an ungainly and technically difficult electrically grounded structure must be inserted inside a hollow electron beam for a distance of about 6 meters.

In order to continue the ion acceleration program by space charge waves a proof of principle experiment is proposed. This experiment utilizes the NRL 50 MeV proton, low intensity cyclotron accelerator as an injector into the space charge wave accelerator. This scheme does, however, not produce an intense energetic ion beam but does test the feasibility of the space charge wave accelerator concept.

The remaining portion of this section presents the progress on the space charge wave accelerator. Figure 7 is a schematic representation of the converging guide type of space charge wave accelerator. In this scheme ions are trapped and accelerated by a negative energy space charge wave traveling on an intense relativistic electron beam. The phase velocity of the wave in a conducting cylinder depends on the ratio of beam to wall radii. The phase velocity increases inversely with this ratio. Thus, the wave can

CONVERGING GUIDE ACCELERATOR

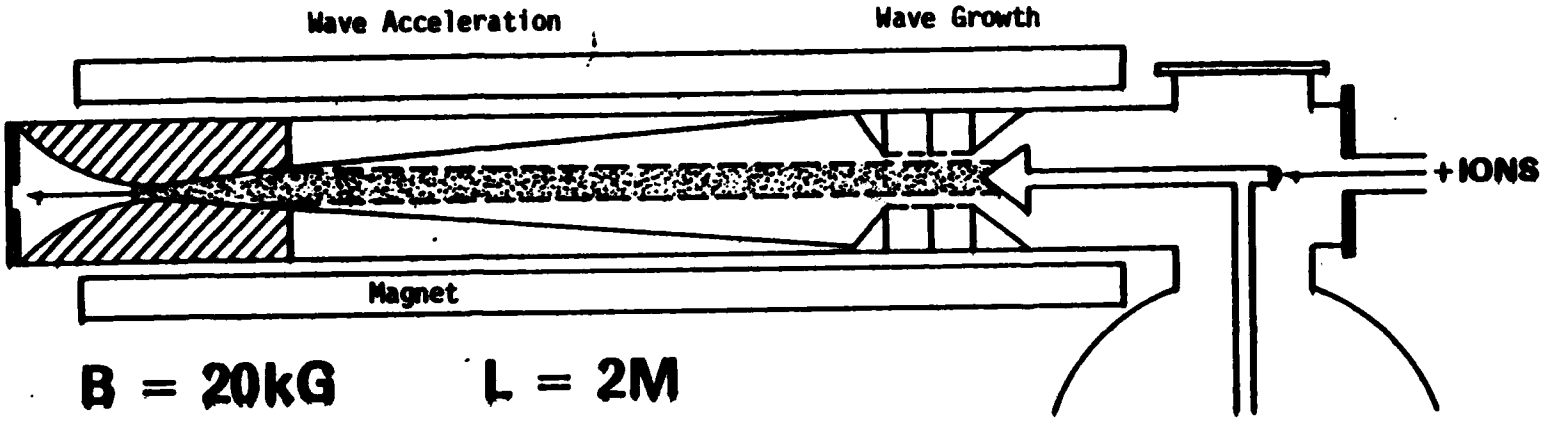

B = 20kG L = 2M

V = 0.5MV

I = 1.4kA

τ = 250 ns

RR = 10pps

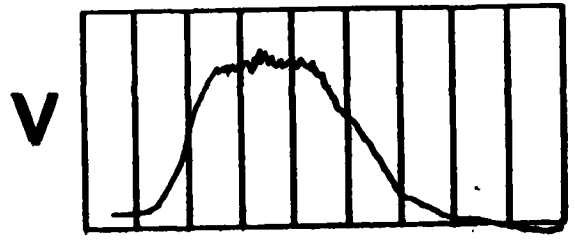

100 ns/DIV

Figure 7
14

be accelerated by accelerating the beam. The beam can be accelerated by passing it through a metal tube with a converging radius.

In Figure 7, ions are injected from the right into the electron beam which is propagating from right to left. Next, a space charge wave is excited and grown around the ions. Now ions loaded into the waves are accelerated by the accelerating wave. The electron beam is then dumped and ions are extracted from the far left. Two meters of magnetic field at a strength of 20 kG are required for this system. The electron beam that is going to be used for this system has an energy of .5 MeV and a current of 1.4 kA for 250 nsec. Also, the electron beam generator is rep-ratable. It can be operated at 10 pulses per second. The current status of the electron beam generator will be presented later in this section. The trace that is shown in Figure 7 is a photograph of the machine voltage vs time. The high voltage machine was used in conjunction with a resistive load.

In order to understand the minimum phase velocity limit one must examine the IREB dispersion relation. Figure 8 is the dispersion relation for an IREB at different ratios of the injected current (I) to the space charge limit current (I_ℓ) of the geometry. I_ℓ is the maximum current that can be transmitted in a given geometry. Considering a wave number of 2 and a ratio of I/I_ℓ of .9, i.e., a +10% change in I/I_ℓ, the phase velocity can increase by about 50%. For higher wave numbers the phase velocity is too high. Ten percent fluctuations on an IREB are realistic as can be seen in Figure 10. However, fluctuations in the diode current can be reduced by inductively integrating the current. This work is currently in progress. Figure 9 is a photograph of the experimental set up. The large tank off to the left of the picture is the high voltage generator and diode section. Figure 10 is a typical diode current trace. The horizontal scale is

IREB DISPERSION

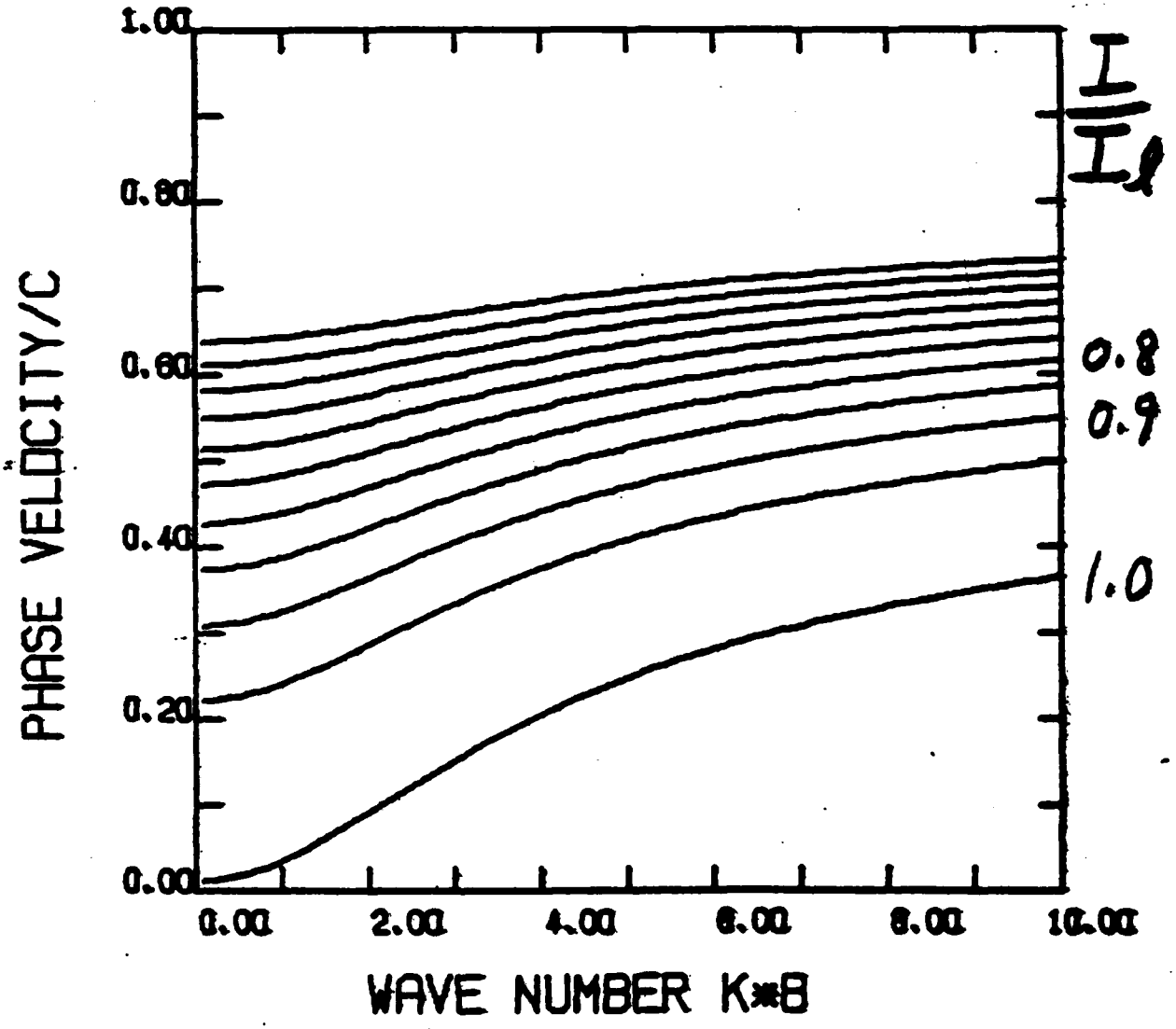

Figure 8

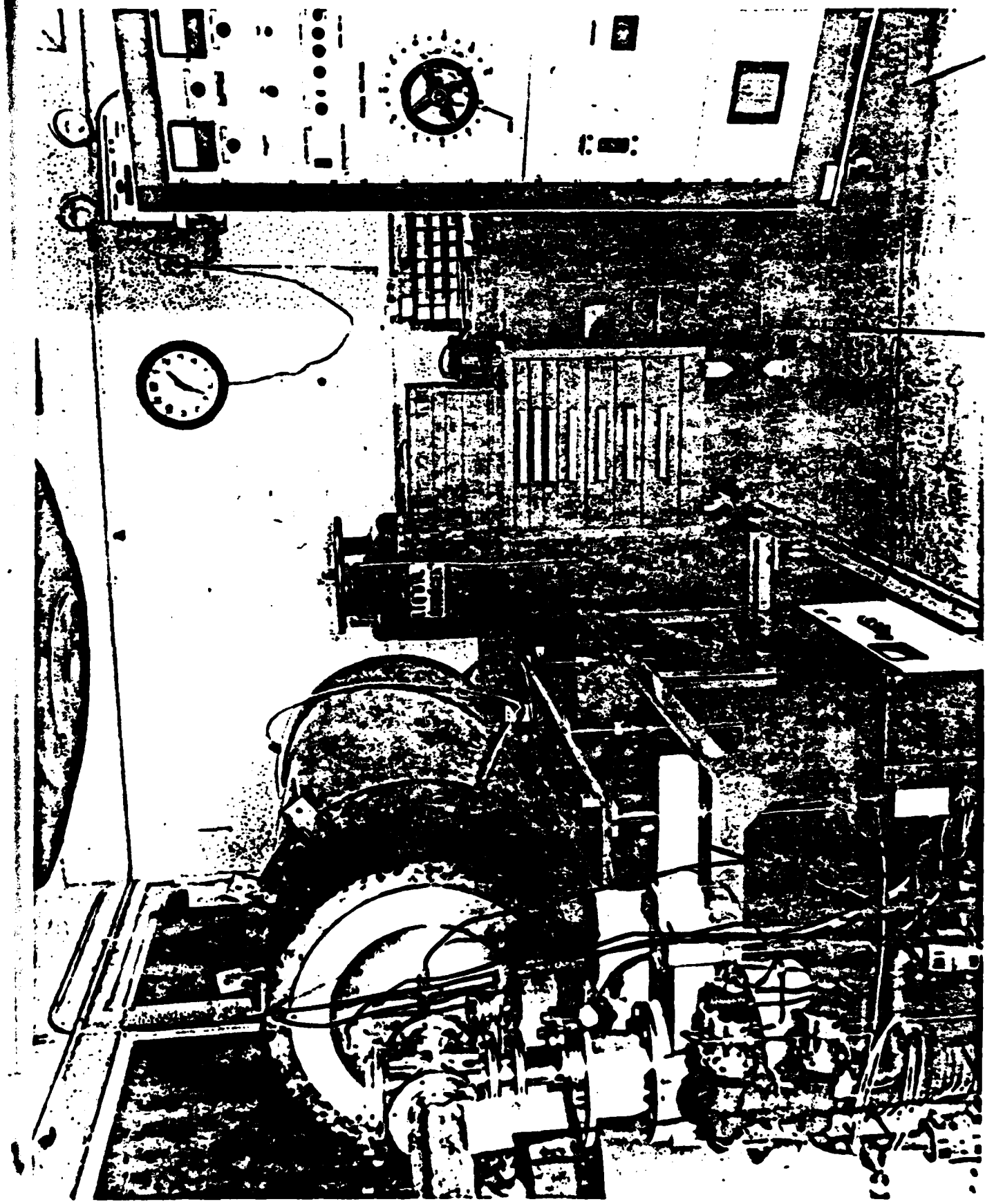

Figure 9

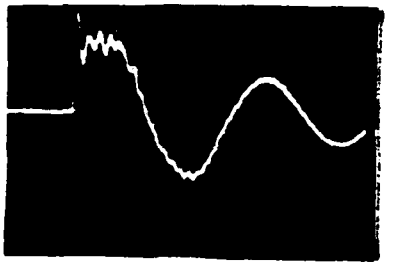

Figure 10

DIODE CURRENT TRACE

Horizontal Scale 200 ns/div
Vertical scale 300 A/div

200 ns/div and the vertical is 300 A/div. After 400 ns of operation the current breaks into an oscillation. This oscillation occurs as a result of shorting between the anode and cathode gap. The diode shorts from closing of the anode-cathode gap by the anode plasma.

Figure 11 shows the damage produced by the beam of electrons on a lucite plate. The plate was located 2 meters from the diode. The electron beam was propagated in a uniform magnetic field of about 3.5 kG. The damage represents the accumulation of damage from 40 shots. The machine was operated at 1 pps. The beam diameter increased by 50% from the injection point.

In summary, we now have an operating electron beam generator. The next stage will be to grow and accelerate waves. Then measure phase velocity and field amplitude. And finally, measure the coherence length of the generated waves.

Completed theoretical and experimental studies have directed the space charge wave accelerator work to a proof of principle experiment.

Figure 11

Damage produced by electron beam on lucite plate. 40 shots @ 1 pps. Beam propagated 2 meters in 3.5 kG field.

A PAPER PRESENTED AT THE 1979 BOSTON APS MEETING

A Foilless Ion Diode. C. Roberson and F. Mako

Naval Research Laboratory--Experimental results from a foilless ion diode capable of repetitive pulsing are presented. More than 10^{14} protons/pulse are observed in a foilless reflexing configuration using an 800 kV, 20 kA, 50 ns electron beam in a 20 kG magnetic field. Both insulating (polyethylene) and conducting (H_2 and D_2 loaded TI) anodes are used. Results on directionability focussing and energy spectrum of the ion beam will be presented.

APPENDIX A

IEEE Transactions on Nuclear Science, Vol. NS-26, No. 3, June 1979

COLLECTIVE ION ACCELERATION CONTROLLED BY A GAS GRADIENT

F. Mako

JAYCOR, Alexandria, VA 22304

A. Fisher, N. Rostoker, D. Tzach

University of California, Irvine, CA 92717

and C. W. Roberson

Naval Research Laboratory, Washington, D.C. 20375

Abstract

Energetic alpha particles are observed when an intense relativistic electron beam is injected into a decreasing pressure profile of helium gas. In a 7 kG external magnetic field up to 10^{10} 9 MeV alpha particles are detected on cellulose nitrate. By viewing the electron beam as an expanding "gas" of reflecting electrons the corresponding ion distribution is calculated and compared to the measured distribution. Good agreement in these results supports the reflecting beam model of Ryutov.

1. Introduction

Graybill and Uglum[1] appear to have first studied collective field acceleration of positive ions due to a relativistic electron beam. The beam was injected into a drift chamber which was uniformly filled with a neutral gas.

Many other experiments[2-5] and theories[6,7,9] have followed and extended this initial investigation. We present experimental results for the case when the external magnetic field is large enough to radially confine the beam.[8] The results are compared with an extended version of the theory proposed by Ryutov.[9]

In this theory, a beam of electrons is confined radially by an external magnetic field. Axially the beam density is confined and allowed to multiply by reflecting alternatively off the cathode and virtual cathode as it passes through a dense plasma filled volume. Ions are accelerated out of the plasma front by the expanding electron "gas."

2. Apparatus

Figure 1 depicts the geometry and diagnostic locations used in the experiment. This figure represents a cross-sectional view of a cylindrical system.

In order to obtain a pressure gradient in the large vacuum chamber, where we require the pressure to be high enough to allow full beam propagation, a fast valve was developed.[10] The vacuum chamber is electrically grounded and made of stainless steel. The beam is formed from a graphite cathode (5 cm dia.) and is injected through a 1 mil thick titanium anode foil. The dashed lines represent the path of the beam.

In this experiment the diode injection conditions were 0.8 MV, 65-70 kA and 60 ns (FWHM). The beam is 5 cm in diameter. Cellulose nitrate film[11] was used to measure the ion energy and number.

3. Experimental Results

Figure 2 is a plot of the maximum helium ion energy against delay time. Delay time is defined to

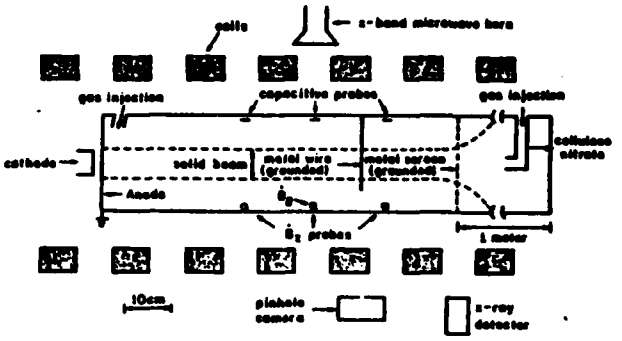

Figure 1. Schematic of experimental set-up.

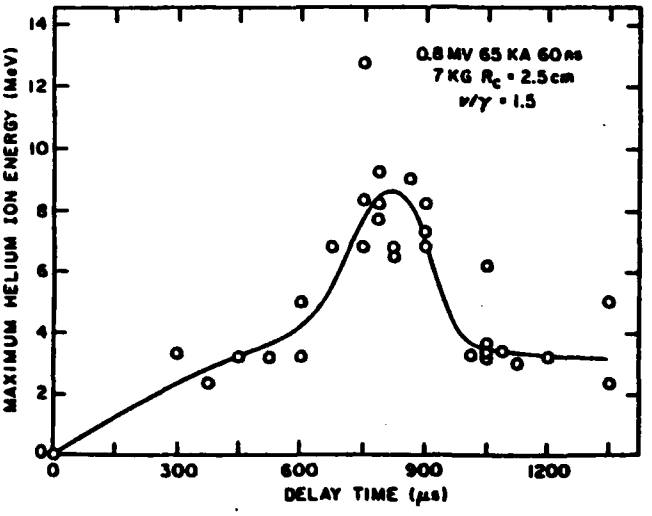

Figure 2. Maximum helium ion energy vs delay time. Each point above 300 μs contains about 10^{10} ions.

be the time that gas is allowed to enter the vacuum chamber before the beam is injected. Figure 3 translates delay time into pressure profile. The number of ions at each point is about 10^{10} (300-1350 μs). This number is measured at 1.7 meters from the anode over the entire cross-sectional area of the chamber (~300 cm^2).

For delay times greater than 1050 μs the pressure is to high over most of the chamber. This results in

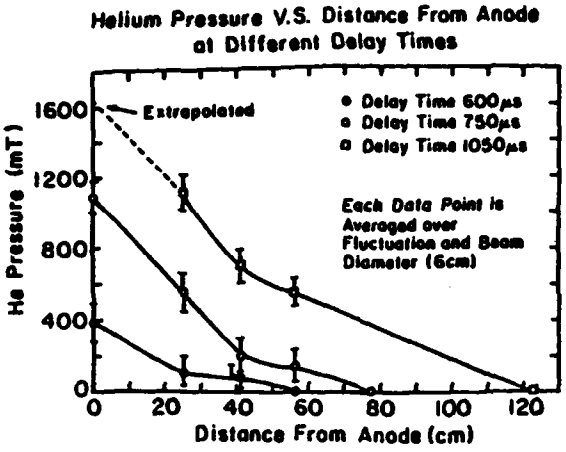

Figure 3. The helium pressure vs distance from anode at three different delay times.

full beam propagation. The forward acceleration of the beam front is too rapid to retain ions.

For delay times below 600 μs only the vacuum limit beam is allowed to propagate. In this region the potential well motion is inhibited by the lack of charge neutralization. Figure 4 illustrates these beam transmission properties.

Under the conditions of maximum ion energy which occurs near 800 μs, most of the transmitted beam is composed of electrons with an energy below 300 keV. A faraday cup covered with titanium foil is used for beam energy and transmission measurements. The foil is used as an energy filter.

The implication being that electrons are axially trapped between the cathode and virtual cathode. These electrons are forced to reflex many times through the anode foil and induced plasma which results in the loss of electron energy parallel to the magnetic field lines.

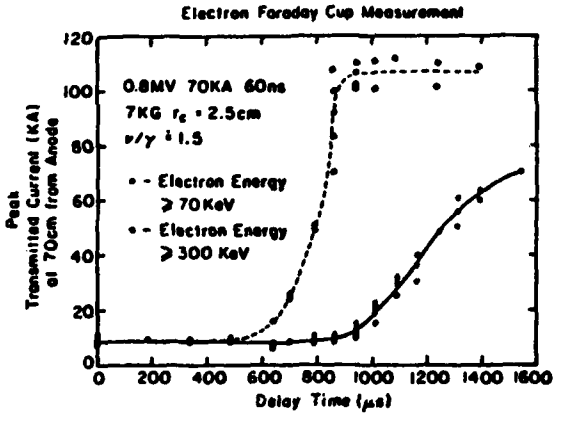

Figure 4. Transmitted beam current vs delay time at different energies.

A simple demonstration of the electrons reflecting is shown by increasing the anode thickness from 1 to 3 mil titanium. This reduces the transmitted low energy (~300 keV) electron current (Figure 5).

4. Theory

The present model extends that of Ryutov[9] by including a description of the potential-electron density relation based on measurements of the transmitted beam current. This model is applicable to the experiment at a delay time of 750-800 μs. Referring to Figure 3. This is so if we consider that the neutral gas from the anode but to 40 cm is a plasma during most of the beam plus length. And by also considering that very little ionization of the gas occurs after a distance of 40 cm from the anode.

We will use a fluid description for the ions:

$$(1) \qquad \frac{\partial n_i}{\partial t} + \frac{\partial}{\partial z}(v_i n_i) = 0$$

$$(2) \qquad \frac{\partial v_i}{\partial t} + v_i \frac{\partial v_i}{\partial z} = -\frac{q}{M}\frac{\partial \phi}{\partial z}$$

where v_i, n_i are the ion velocity and density, respectively, q, M are the ion charge and mass, respectively. ϕ is the electrostatic potential, z is the axial position coordinate with its origin at the plasma front, t is the time coordinate.

Equations (1) and (2) will be closed by the potential-electron density relation and the assumption of quasi-neutrality.

By making use of a generalized form for the definition of current density, which allows for currents of different energy,

$$(3) \qquad n_e = \frac{-2}{e}\int \frac{(dJ/dE)\,dE}{v}$$

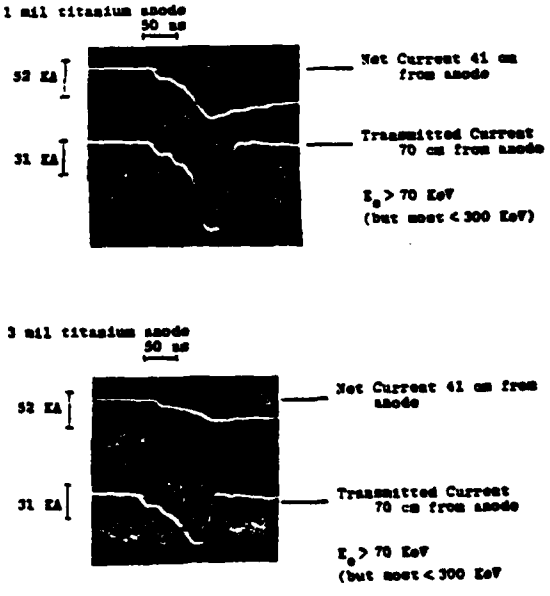

Note: Delay Time 863 μs Helium

Figure 5. Reduction of low energy reflexing electrons by increasing anode thickness.

the potential-density can then be determined.

Where e is the electron charge, E is the parallel (to the magnetic field lines) electron energy, v is parallel electron velocity, J(E) is the current density with electron energy E. The factor of 2 accounts for total reflection of the electron density.

From the two data points for the transmitted current at 800 μs (Figure 4), the shape of J(E) is strongly suggested. This data and assuming J(E) is monatonic is used to construct J(E).

We will assume that J(E) has the following form:

$$(4) \qquad J(E) = J(0)\left[1 - \frac{E}{E_{max}}\right]^{\alpha} \quad ,$$

where J = I/A, I(E) is the transmitted current and A is the cross-sectional area of the beam. α is determined by picking I = 8 kA at 300 keV. This gives α = 3.4.

By using the non-relativistic energy conservation relation for electrons and substituting Eq. (4) in (3), the integration can be completed.

$$(5) \qquad n_e = n_o(1 + \phi/\phi_o)^{5/2} \quad ,$$

$$\text{where } n_o = \frac{16}{5}\,\frac{I(0)}{eA}\sqrt{\frac{2m}{E_{max}}}$$

and ϕ_o is the cathode potential, m is the electron mass. To simplify the integration α = 3 was used.

We will now determine the self-similar solution of Eqs. (1), (2), and (5) by making use of the definitions,

$$U \equiv v_i/v_o \quad , \quad N \equiv n_i/n_o \quad , \quad \psi \equiv \phi/\phi_o \quad , \quad v_o \equiv \sqrt{\frac{q\phi_o}{M}}$$

and $\zeta \equiv z/v_o t$,

The solution is completely determined when the conservation of energy at the plasma front is used. That is:

$$\frac{U^2}{2} + \psi = 0 \quad \text{at} \quad z = 0$$

Now the ion number-energy relation can be computed and is

$$(6) \qquad N_i(E_i) = \frac{n_o A}{\beta}\left[\sqrt{\frac{6}{5}} - \sqrt{\frac{E_i}{5q\phi_o}}\right]^6 \quad ,$$

where $N_i(E_i)$ is the number of ions with energy E_i and

$$\beta \equiv \sqrt{\frac{5}{2}}\,\frac{1}{v_o t} \quad .$$

By picking the experimental numbers: t = 100 ns I(0) = 40 kA and E_{max} = 800 keV for He^{++}, the natural logarithm of Eq. (6) can then be compared to the measured results. (See Figure 6.) The data has been corrected for the loss of ion energy ($q\phi_o$) at a grounded detector.

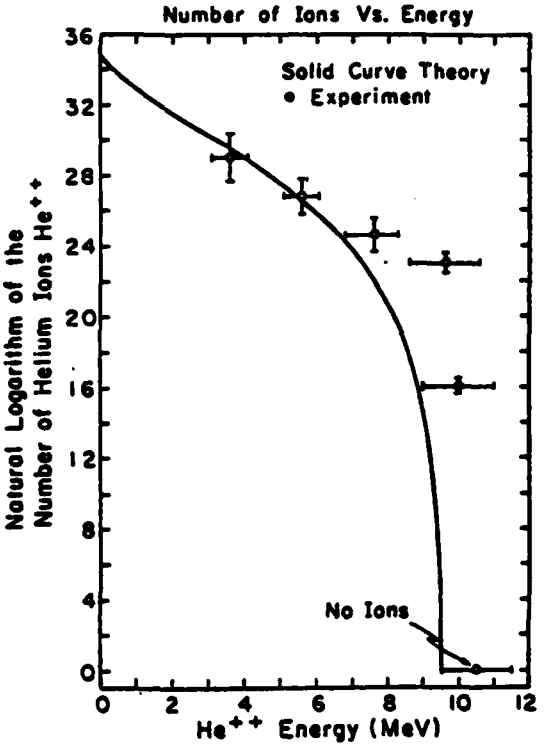

Figure 6. Comparison between theory and experiment of the natural logarithm of the number vs energy relation.

5. Summary and Conclusions

The reflecting beam model initially proposed by Ryutov[9] has been extended and used to predict the ion energy distribution subject to the constraints of the beam current-energy distribution. The predictions compare with the data quite favorably in a limited parameter regime.

The ion acceleration may be extendable to higher energies if thinner anode foils are used along with stronger external magnetic fields. These modifications would allow for more electron reflecting and a greater electron density.

References

1. S. E. Graybill and J. R. Uglum, J. Appl. Phys. 41, 236, 1970.
2. B. Ecker, S. Putnam and D. Drickey, IEEE Trans. N.S. 20, 301, 1973.
3. G. W. Kuswa, L. P. Bradley, and G. Yonas, IEEE Trans. N.S. 20, 305, 1973.
4. S. E. Graybill, IEEE Trans. N.S. 19, 292, 1972.
5. G. W. Kuswa, Annals of the New York Academy of Sciences, 251, 514, 1975.
6. C. L. Olson, Annals of the New York Academy of Sciences, 251, 536, 1975.
7. S. D. Putnam, Phys. Rev. Lett. 25, 1129, 1970.
8. F. Mako, Ph. D. Thesis, to be published.
9. D. D. Ryutov, G. V. Stupakov, Fizika plazmy, 2, No. 4 and 5, 1976.
10. A. Fisher, F. Mako, and J. Shiloh, Rev. Sci. Instrum 49(6), 872, 1978.
11. R. L. Fleischer, P. B. Price, and R. M. Walker, Nuclear Tracks in Solids, Univ. of Calif. Press (1975).

APPENDIX B

IEEE Transactions on Nuclear Science, Vol. NS-26, No. 3, June 1979

COLLECTIVE ION ACCELERATION WITH AN INTENSE REB IN A PERIODIC WAVEGUIDE

P. Sprangle,* C. W. Roberson,*
and Cha-Mei Tang+

Abstract

A scheme to collectively accelerate ions from 1.0 MeV to 30 MeV using a higher order spatial harmonic of a variable period slow wave structure is described.

Introduction

According to recent calculations it may be possible to collectively accelerate ions in the potential well of space charge waves to GeV energies with field strengths as large as 1 MeV/cm using a converging guide accelerator.[1]

However, it is difficult to obtain very low initial phase velocities in such an accelerator, unless the current is very close to the limiting current for beam propagation. Hence, the converging guide accelerator requires an ion injection energy in excess of 30 MeV. In this paper the acceleration of ions from 1.0 MeV to 30 MeV using the n = 1 spatial harmonic of a variable length periodic slow wave structure is discussed. This accelerating configuration utilizes a periodically loaded waveguide to effectively reduce the phase velocity of a negative energy space charge wave. In the absence of the periodic structure the phase velocity of the space charge wave is close to the electron beam velocity. The periodic structure, however, "rectifies" the wave thus producing spatial harmonics. The first harmonic has a phase velocity of $v_{ph,1} = \omega/(k + 2\pi/L(z))$ where ω and k are the frequency and wave number of the fundamental wave and L is the period associated with the structure. For L sufficiently small the phase velocity, $v_{ph,1}$, can be made equal to the velocity of the background ions, thus trapping the ions. The trapped ions are now gradually accelerated by slowly increasing the period as a function of axial distance down the guide.

The relativistic electron beam excites and provides the energy to the waves which accelerates the ions. The zero order potential well due to the space charge provides radial confinement of the ions. The periodic wall accelerator can be designed so that protons of 1.0 MeV from an ion diode connected to a pulse line driven by a Marx generator are in resonance with the n = 1 spatial harmonic only. Hence, the ions see the other harmonics as rapidly varying fields.

In this paper the results from calculations of the dispersion relation, limiting current, maximum accelerating field and a discussion of an experimental configuration are presented.

Analysis of Periodic Wall Accelerator

The slow wave structure is shown in Fig. 1; in this model the electron beam is assumed to be infinitesimally thin, $\Delta r \to 0$, and constrained to move solely in the axial direction. All wave and beam quantities are taken to be independent of the spatial variable y. We further assume that the wavelength of the fundamental wave on the beam is much greater than the opening of the slot, ℓ_o. The fields within the slots are approximated to be independent of z. From Maxwell's equations and the equation of motion we can determine the space and time dependence of the z component of the electric field in the three regions of figure 1 and the axial linear response current of the beam. Applying the boundary conditions we find the dispersion relation and the ratio of the field amplitudes. The dispersion relation for the system depicted in Fig. 1 is

$$\cot\left(\frac{\omega}{c}X_{21}\right) = \sum_{n=-\infty}^{\infty} \frac{\omega/c}{q_n}\alpha_n^2 \frac{\cosh(q_nX_1) - \Delta X q_n (p_n/q_n)^2 \sinh(q_nX_o)\cosh(q_nX_{10})}{\sinh(q_nX_1) - \Delta X q_n (p_n/q_n)^2 \sinh(q_nX_o)\sinh(qX_{10})} \quad (1)$$

where $\alpha_n^2 = (\ell_o/L)(\sin(k_n\ell_o/2)/(k_n\ell_o/2))^2$; n = 0, ±1, ±2...; $k_n = k + 2\pi n/L$, k is the fundamental wave number; $q_n^2 = k_n^2 - \omega^2/c^2$; $p_n^2 = -q_n^2\left[1 - (\omega_b^2/\gamma_e^3)/(\omega - V_e k_n)^2\right]$; $\omega_b^2 = 4\pi|e|^2 N_o/M_o$, N_o is the local beam density; $\gamma_e = (1 - \beta_e^2)^{-\frac{1}{2}}$, $\beta_e = V_e/c$.

To write the dispersion relation in a manageable form we make some simplifying assumptions. If we consider wavelengths much greater than the periodicity, i.e. $k \ll 2\pi/L$. This allows to neglect all but the n = 0 term on the right hand side of Eq. (1). This result can be used as an iteration to find $k_1 = k + 2\pi/L$.

It can be shown from limiting current arguments that

$$\Delta X X_o \omega_b^2/\gamma_e^3 c^2 = \xi X_2/X_{20} \quad (2)$$

where $\xi = R\beta_e^2(\beta_L\gamma_L/\beta_e\gamma_e)^3 \leq 1$, $R = I_e/I_L$ is the ratio of the beam current to the limiting current, $X_{20} = X_2 - X_o$ and $\gamma_L = (1 - \beta_L^2)^{-\frac{1}{2}}$ is the limiting beam gamma.

Using Eq. (2) and the low frequency approximations, i.e. $|qX_1| \ll 1$, $\omega X_{21}/c \ll 1$, $k\ell_o/2 \ll 1$. The dispersion relation can be written as

$$(\delta k - \delta k_1)(\delta k - \delta k_2) = -\delta k_1 \delta k_2 X_o/X_{10} \quad (3)$$

where $\delta k = k - \omega/V_e$, $\delta k_2 = \frac{1}{2}\frac{\ell_o}{L}\frac{\omega}{c}\frac{X_{21}}{X_1}$ and $\delta k_1 = 2\xi\frac{\omega}{c}\frac{X_2}{X_{20}}\frac{X_{10}}{X_1}$. The dispersion relation in (3) is valid in the limit $V_e \approx c$, $|\delta k| \gg \omega/(2\omega\gamma_e^2)$ and $\omega_b^2/\gamma_e^3(\omega - V_e k)^2 \gg 1$.

With the above approximations we find the ratio of the first order harmonic to the zero order harmonic to be

$$\frac{E_{z,1}}{E_{z,o}} \approx \frac{X_1}{X_o}\frac{\sinh(2\pi X_o/L)}{\sinh(2\pi X_1/L)}\frac{\sin(\pi\ell_o/L)}{\pi\ell_o/L}(\delta k - \delta k_1)/\delta k \quad (4)$$

*Naval Research Laboratory, Washington, D.C. 20375
+Jaycor, Alexandria, Virginia

The maximum accelerating electric field is reached when the electrons of the beam begin to trap in the fundamental (n = 0) electric field component of the wave. The onset of trapping occurs when the axial electric field reaches the value

$$E_{z,o} = \gamma_o^3(\omega - V_o k)^2 \frac{M_o}{|e|k} \sim \gamma_o^3 \frac{\delta k^2}{k} \frac{M_o c^2}{|e|} \qquad (5)$$

As an example let us consider the parameter regime $\delta k_1 \ll \delta k_2$. This decouples the slow beam and electromagnetic mode, the dispersion relation then becomes

$$\delta k = \delta k_1 X_1 / X_{10} \qquad (6)$$

where ζ must satisfy $X_{20}/4\gamma_o^4 X_2 \ll \zeta \ll$ $\beta_o^2 X_{21} X_{20}/4 X_{10} X_2$. Then Eqs. (4) and (5) become

$$\frac{E_{z,1}}{E_{z,0}} = \frac{\sin(\pi \ell_o/L)}{(\pi \ell_o/L)} \frac{\sinh(2\pi X_o/L)}{\sinh(2\pi X_1/L)} \qquad (7)$$

and

$$E_{z,o} = 4\gamma_o^3 \zeta^2 \frac{(\omega/c)^2}{k} \frac{X_2}{X_{20}}^2 \frac{M_o c^2}{|e|} \qquad (8)$$

As an example let $\ell_o/L = \frac{1}{2}$, $X_o = 1$ cm, $X_1 =$ 1.2 cm, $X_2 = 3.0$ cm and $X_{20} = 2$, these values give $E_{z,1}/E_{zo} = 0.28$. The maximum field due to trapping for $\gamma_o = 5$, $L = 1.5$ cm, $\zeta = 1/10$, $V_{ph}/c = 1/20$ is $\sim$ 1.2 MeV/cm. Hence, the accelerating wave has the magnitude, $E_{z1} = 0.33$ MeV/cm.

The calculations have been carried out in cartesian coordinates; however, the results are approximately correct for a cylindrical system with a small aspect ratio. To accelerate ions from 1.0 MeV to 30 MeV in resonance with the first spatial harmonic using a frequency of 1 GHz requires an initial period of 1.5 cm and a final period of 8.0 cm. The rate of change of the structure and the total length are determined by the maximum E_z field where the ions are trapped. As an example the accelerating field as determined from Eqs. (7) and (8) is about 0.33 MeV/cm and the minimum length would be $\sim$ 1M. A more practical limit, based on electron linear accelerators is about 200 KV/cm for the fundamental. This would give a minimum length of $\sim$ 6M.

1. P. Sprangle, A. T. Drobot, and W. M. Manheimer, Phys. Rev. Lett., 36, 1180 (1976).

Varying Period Slow Wave Structure